buildings

MDPI

Article

Numerical Study on Mechanical Characteristics of Tower Sections with Main Member Disconnection

Hengwei Zheng *, Changli Wu, Jinhong Liu, Lang Zhong, Kai Li and Zhitao Yan

Department of Theoretical and Applied Mechanics, Chongqing University of Science and Technology, Chongqing 401331, China; 2021206013@cqust.edu.cn (C.W.); 2021206054@cqust.edu.cn (J.L.); 2021206046@cqust.edu.cn (L.Z.); 2023206099@cqust.edu.cn (K.L.); 2016023@cqust.edu.cn (Z.Y.)
* Correspondence: zhenghw@cqust.edu.cn

Abstract: Restricted by the existing construction technology, there are a lot of disconnections in the angle steel components of transmission towers. At present, there are more studies on single angle steel or cross bracing, but less on the main member containing disconnection joints. According to the disconnection position in the main member, an upper end disconnection, middle end disconnection, and lower end disconnection were designed in this paper. At the same time, a tower section model of a connected main member and a tower section model of a disconnected main member were established and analyzed by finite element analysis. Considering the loadings acting on transmission towers, the two load conditions of axial loading and tension–compression coupling are set. Considering the loadings acting on transmission towers, the influences of the combination form of the inner and outer steel cladding and the steel cladding area ratio on the ultimate bearing capacity of the main member were studied under 72 groups of different tower sections applied with axial loadings. The influence of the disconnection joints on the stability of the tower section was studied under 24 groups of different tower sections applied with tension and compression coupled loading conditions. Referring to the specifications, the slenderness ratio correction factor formula of the disconnect main member can be derived. The results indicate that when designing the disconnection joint in the main member, it is recommended to choose a middle end disconnection with a steel cladding area ratio of 1.0.

Keywords: disconnection joint; tower section; ultimate bearing capacity; slenderness ratio correction factor

Citation: Zheng, H.; Wu, C.; Liu, J.; Zhong, L.; Li, K.; Yan, Z. Numerical Study on Mechanical Characteristics of Tower Sections with Main Member Disconnection. *Buildings* **2024**, *14*, 2998. https://doi.org/10.3390/buildings14092998

Academic Editor: Tomasz Sadowski

Received: 21 July 2024
Revised: 13 September 2024
Accepted: 19 September 2024
Published: 21 September 2024

1. Introduction

Due to the advantages of low cost and easy installation, angle steel transmission towers are widely used in practical engineering. A transmission tower is composed of a tower top, a tower body, and tower legs. In this paper, a tower section was selected from the tower body as the object in order to analyze the influence of main member disconnection joints on its mechanical properties. A transmission tower section contains two main members, one cross bracing, and several auxiliary support members. The stable bearing capacity of equilateral angle steel as the main load-bearing component of transmission towers is always a research focus. Experts and scholars usually treat equilateral angle steel main members as axially compressive bars and have studied their stable bearing capacity by using axial compression tests, finite element simulation analysis, or theoretical calculations [1–7]. Some experts also analyzed the mechanical characteristics of the main members by studying the entire tower [8–12].

Restricted by the existing construction technology, there are a lot of disconnections in the angle steel components of transmission towers, and their location is usually in the main member at the bottom of the tower section. The disconnected joints are connected by bolts and steel cladding. Currently, the relevant codes in the field of transmission towers only specify requirements for the length of disconnecting joints, the number of bolts, and the steel cladding area, which are considered relatively conservative [13,14]. Therefore,

there is a necessity to conduct further research on disconnecting joints in main members. Few studies have focused on this area. According to Gao [15], the steel cladding area in disconnecting joints has an impact on joint stiffness, and he also studied the layout position of disconnecting joints. Xue [16] examined disconnecting joints of various sizes in main members. However, while many scholars have studied the mechanical properties of bolted connection nodes in transmission towers [17–22], there is relatively little research on the main member disconnection joints. The disconnection of the main member will influence the stability of the tower section. Scholars have conducted extensive research on the out-of-plane instability and the corresponding laws of the intact tower section's cross bracings through experiments and finite element simulations [23–26], but there is relatively little research on tower sections with main member disconnection.

Although domestic and foreign scholars have conducted extensive research on the bearing capacity of main members and the stability of cross bracing, when considering the interaction between the main member, cross bracing, and auxiliary support member, there is relatively little research on the mechanical responses of a tower section with main member disconnection from the perspective of the overall structure. In this paper, INVENTOR was utilized to establish tower section models of both an intact main member and a main member with disconnection. Then, the mechanical responses of these models were studied using a numerical method. The slenderness ratio correction factor formula of the disconnected main members was derived. Therefore, there is significant reference value in optimizing the design of main member disconnection joints in practical engineering.

2. Materials and Methods

2.1. Principle of Slenderness Ratio Correction of Main Members

The slenderness ratio is an important parameter for describing the stability of a member. For the main member, the disconnection joint will directly affect its stable bearing capacity. The slenderness ratio of the main member containing the disconnection joint can be obtained by reverse calculation of its ultimate bearing capacity. In this paper, the ultimate bearing capacity of the disconnected main member was obtained through finite element calculation, and then the slenderness ratio of the disconnected main member was calculated by combining it with the stable bearing capacity calculation method for axial compression components [23] (derived from: Technical code for the design of tower and pole structure of overhead transmission lines DL/T 5154-2012). The slenderness ratio correction factor is derived by comparing the slenderness ratio of disconnected main members with that of connected main members. The following formula for calculating the bearing capacity of axially compressed components has been provided in standard DL/T 5154-2012 [23]:

$$N/(\varphi \cdot A) \leq m_N \cdot f \tag{1}$$

Here, N is axial tension or axial pressure; φ is the stability coefficient of axially compressed components; A is the gross cross-sectional area of the component; m_N is the reduction coefficient of the stable strength of the compression bar; and F is the design value of the steel strength of the component.

The calculation steps for the slenderness ratio of the disconnected main member are as follows:

(1) Substitute the ultimate bearing capacity of each disconnected main member obtained from the finite element calculation into formula (1) to deduce the stability coefficient of the compression φ.
(2) Calculate the corrected slenderness ratio based on the stability coefficient φ value table provided in reference to DL/T 5154-2012.
(3) The slenderness ratio correction coefficient K_λ of the main member can be obtained by dividing the corrected slenderness ratio λ_n derived from step (2) by the nominal slenderness ratio, as shown in Equation (2).

$$K_\lambda = \lambda_n / \lambda \tag{2}$$

2.2. Tower Section Model

2.2.1. Tower Section Structure and Disconnection Design

In this paper, a tower section of an equilateral angle steel transmission tower was selected in a certain high-voltage transmission project as the object with which to study a main member disconnection joint. The structure of the tower section and the dimensions of the components in the structure are shown in Figure 1. The main member and the joint steel cladding are made of Q420 (nominal yield strength = 420 MPa), and the cross bracing and auxiliary support members are made of Q235 (nominal yield strength = 235 MPa). According to the position of the main member disconnection joint within the tower section, three types of main member disconnection joints were designed: upper end disconnection, middle end disconnection, and lower end disconnection. At the same time, a model of the connected main member was designed as the control group, as shown in Figure 2.

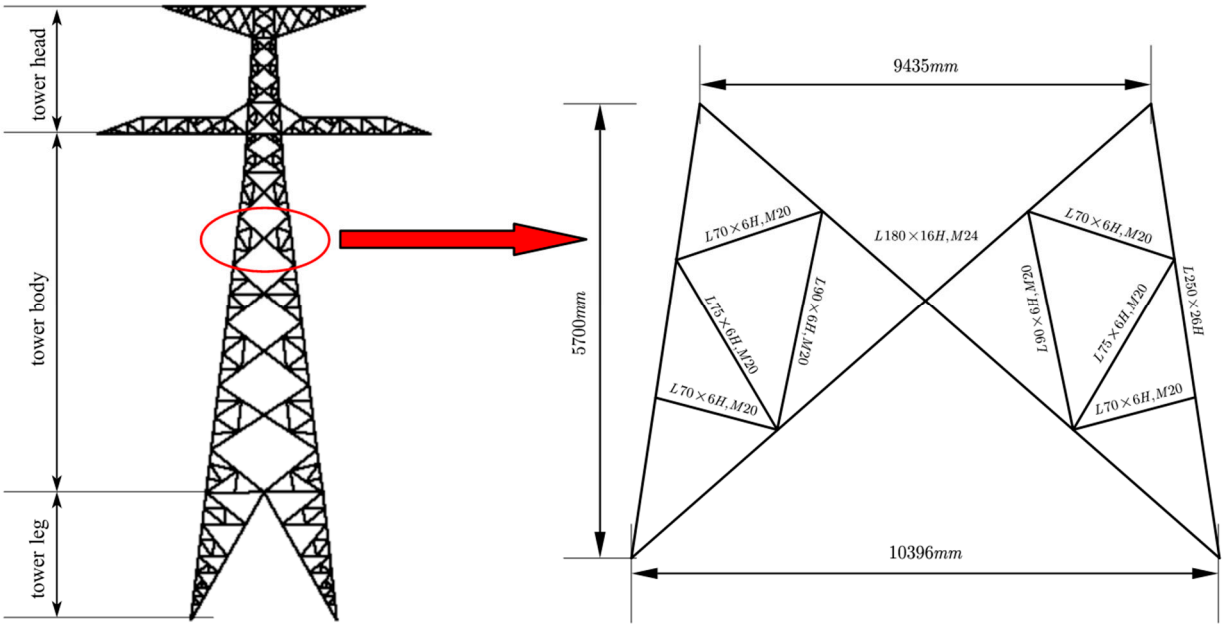

Figure 1. Tower section structure diagram.

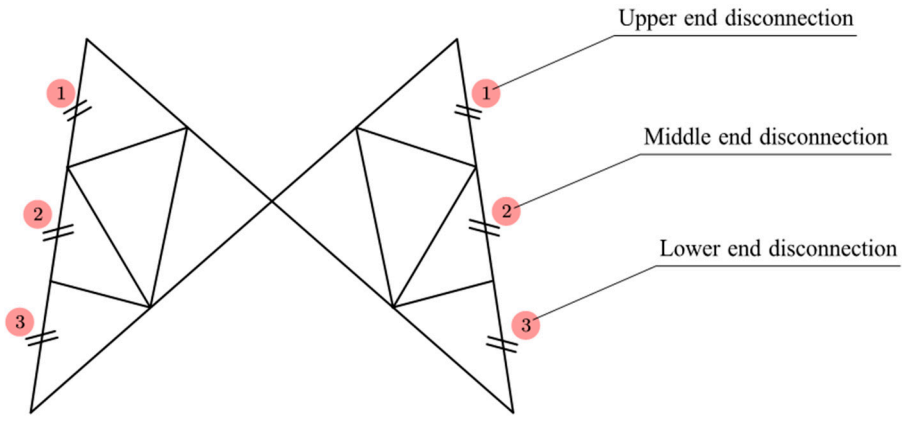

Figure 2. Schematic diagram of tower section disconnection design.

2.2.2. Main Member Disconnection Joints

The external pasting and the internal cladding bolt connection are applied to the main member disconnection joints. The bolts on the joint are uniformly M24 bolts and are arranged in a staggered manner according to the requirements of GB50017-2017 "Code for Design of Steel Structures" [24], as shown below in Figure 3. Here, in Figure 3b, A is

the internal steel cladding of the joint, B is the main member, and C is the external pasting plate of the joint. The internal steel cladding and the external pasting plate are collectively referred to as the steel cladding. The ratio of the steel cladding area is defined based on the ratio of the cross-sectional area of the steel cladding to the cross-sectional area of the main member, and the calculation formula is as follows:

$$a = \frac{A_b}{A_0} \tag{3}$$

Here, A_b is the gross cross-sectional area of the steel cladding and A_0 is the gross cross-sectional area of the main member.

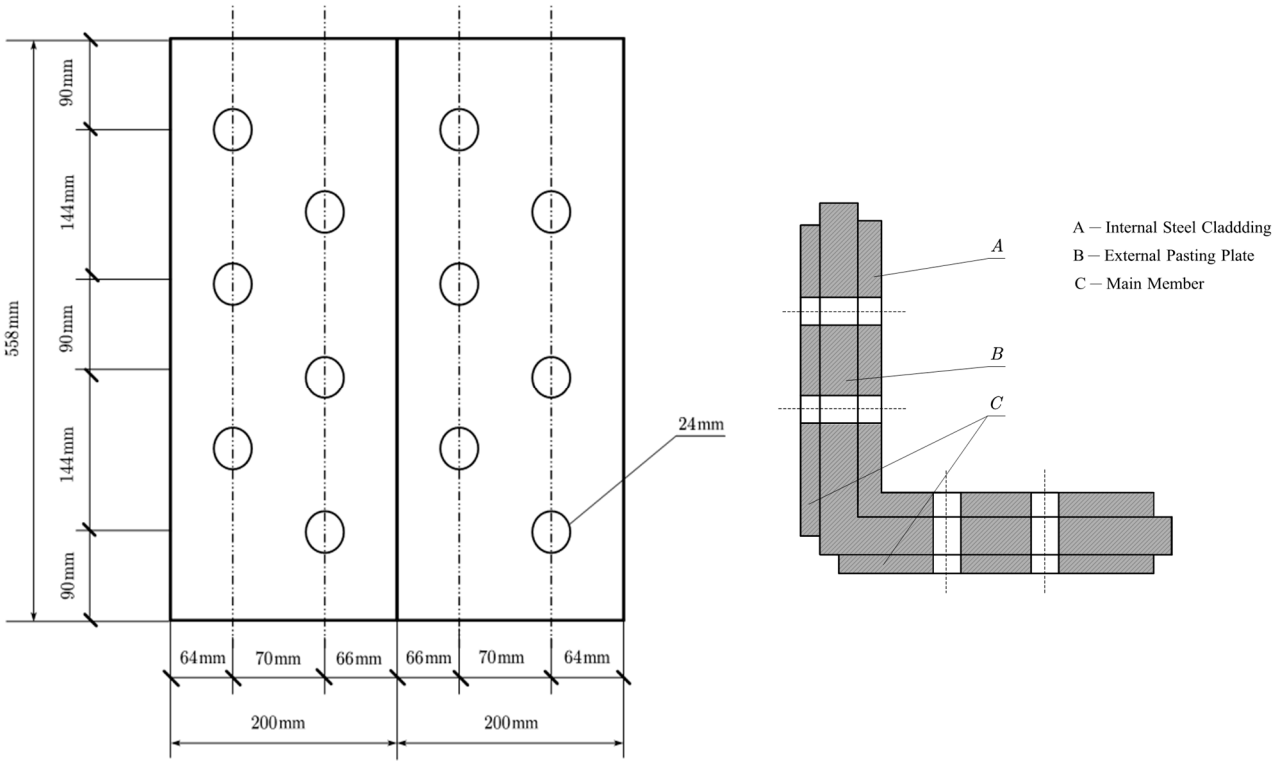

(**a**) Internal steel cladding joint bolt layout diagram. (**b**) Joint cross-section diagram.

Figure 3. Main member disconnection joint.

In this paper, the disconnection joint was taken as an important research object and the area ratio of the steel cladding was studied as the main control variable. Six different steel cladding area ratios were set: 0.8, 0.9, 1.0, 1.1, 1.2, 1.3. Four different combinations of inner and outer steel cladding were given by comparing the steel cladding area ratios of each group, as shown in Table 1. Due to the characteristic of the steel cladding area ratio, the actual calculated steel cladding area ratio cannot be accurately determined as the design value of the steel cladding area ratio. Therefore, an approximate actual steel cladding area ratio is selected for calculation during the calculation process.

Table 1. Steel cladding design for disconnection joints.

Design Steel Cladding Area Ratio	Number	Internal Steel Cladding (mm)	External Pasting Plate (mm)	Main Members (mm)	Actual Steel Cladding Ratio
0.8	A1	L200 × 11	198 × 15	L250 × 26	0.83
	A2	L200 × 13	198 × 13	L250 × 26	0.83
	A3	L200 × 15	198 × 11	L250 × 26	0.82
	A4	L200 × 18	198 × 8	L250 × 26	0.82
0.9	B1	L200 × 14	198 × 15	L250 × 26	0.92
	B2	L200 × 15	198 × 14	L250 × 26	0.92
	B3	L200 × 16	198 × 13	L250 × 26	0.92
	B4	L200 × 17	198 × 12	L250 × 26	0.91
1.0	C1	L200 × 15	198 × 17	L250 × 26	1.01
	C2	L200 × 16	198 × 16	L250 × 26	1.01
	C3	L200 × 17	198 × 15	L250 × 26	1.01
	C4	L200 × 18	198 × 14	L250 × 26	1.01
1.1	D1	L200 × 15	198 × 20	L250 × 26	1.14
	D2	L200 × 16	198 × 19	L250 × 26	1.11
	D3	L200 × 17	198 × 18	L250 × 26	1.11
	D4	L200 × 18	198 × 17	L250 × 26	1.10
1.2	E1	L200 × 13	198 × 25	L250 × 26	1.21
	E2	L200 × 14	198 × 24	L250 × 26	1.21
	E3	L200 × 16	198 × 22	L250 × 26	1.21
	E4	L200 × 17	198 × 21	L250 × 26	1.20
1.3	F1	L200 × 14	198 × 28	L250 × 26	1.34
	F2	L200 × 16	198 × 26	L250 × 26	1.33
	F3	L200 × 18	198 × 24	L250 × 26	1.33
	F4	L200 × 21	198 × 21	L250 × 26	1.32

2.2.3. Load Conditions

Considering the mechanical characteristics of transmission towers, two tower section load conditions were designed. The first load condition is shown in Figure 4a, as the main load-bearing component of the transmission tower; the axial loading applied to the main member of the tower section serves to simulate the vertical loading of the transmission tower. The second load condition is shown in Figure 4b. The most important role of the transmission tower is to support the overhead transmission line; therefore, the application of tension–compression coupling loads to the tower section serves to simulate the transverse load of the transmission tower.

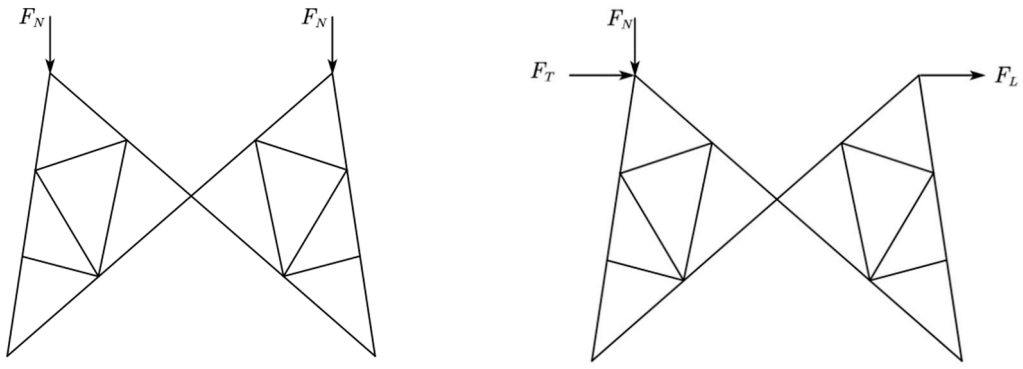

(**a**) Condition1: Axial load. (**b**) Condition2: tension and compression coupling load.

Figure 4. Two load conditions.

2.2.4. Finite Element Model

Combining 3D modeling and finite element analysis in this study, the tower sections were modeled and conducted by finite element simulation analysis. The 8-node 3-dimensional solid element can accurately describe the deformation of the structure and possesses the advantages of good convergence performance and computational stability. Therefore, the 8-node 3-dimensional solid element is used to mesh the tower section models, with a 20 mm swept grid size applied to the models, and the grid is refined at the bolt positions. To enhance the precision and accuracy of the finite element analysis, the mesh at the bolt-hole positions and breaking node locations is refined. Since bolt connections are not the focus of this paper, we utilize the multipoint restraint and beam element simulation bolts to establish the connections between members. The yield strength of the Q420 steel used is 420 MPa, and the elastic modulus and Poisson's ratio are 2.06×10^5 MPa and 0.28, respectively. The yield strength of the Q235 steel used is 235 MPa, and the elastic modulus and Poisson's ratio are 2.1×10^5 MPa and 0.27, respectively. As the angle steel components of the transmission tower are made of steel, the ideal elastoplastic model is selected as the constitutive model for the steel according to the material properties test in Reference [27], as shown in Figure 5. According to the tower section model test device described in Reference [27], the boundary conditions are constrained in terms of both the translational degrees of freedom (in the X, Y, and Z directions) and the rotational degrees of freedom (UR1 and UR3) at the non-loading end at the bottom of the model. The tower section is loaded according to the specified loading conditions, and the loading adopts a gradual incremental method. The load continues to increase until the stiffness matrix of the entire structure becomes singular and can no longer converge iteratively, at which point the load is determined to be the ultimate bearing capacity. In the nonlinearity settings, geometric nonlinearity is enabled. The connection tower section finite element models are shown in Figure 6.

The ultimate bearing capacity of the connection main member will be calculated using two methods. One method was to use formula (1) to calculate the ultimate bearing capacity as a theoretical value of 4052.9 kN; the other method was to calculate the ultimate bearing capacity as a numerical value of 4669.5 kN by finite element analysis. Analysis of the error between the theoretical and finite element results shows that the relative error is 12.21%, which is considered relatively small. Therefore, it is feasible to use the finite element method to simulate the loadings acting on the main member. The finite element model of the tower section with main member disconnection is presented in Figure 7, where the grid refinement at the connection joint positions has been implemented.

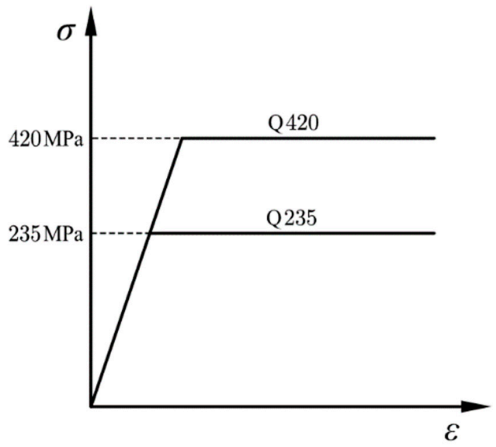

Figure 5. The ideal elastoplastic model.

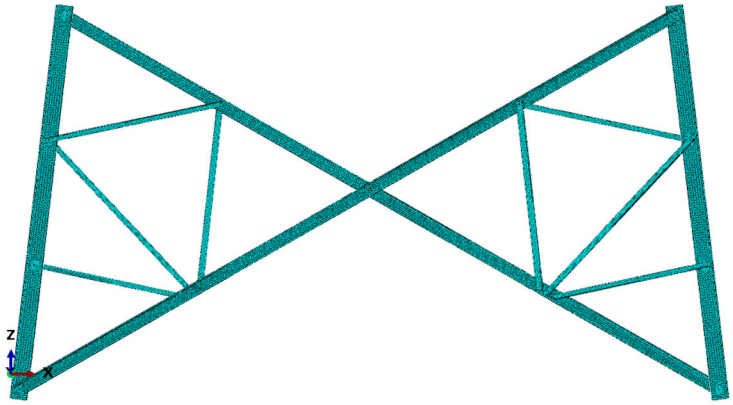

Figure 6. Connection tower section finite element model.

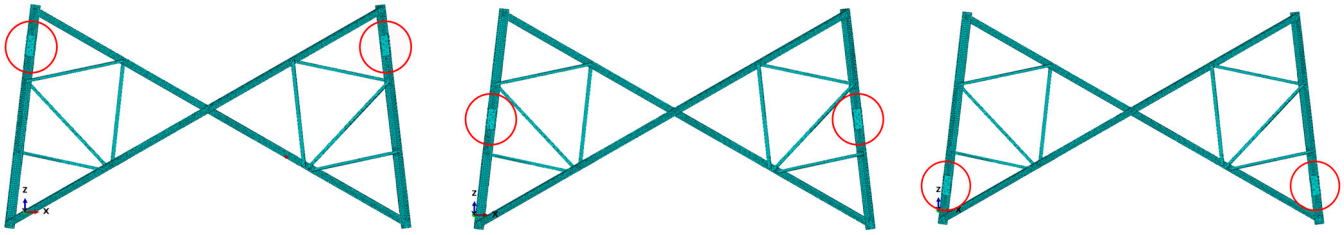

(**a**) Upper end disconnection. (**b**) Middle end disconnection. (**c**) Lower end disconnection.

Figure 7. Disconnection tower section finite element model. (The disconnection joint is in the red circle).

3. Results and Discussion

3.1. Analysis of Finite Element Results for Axial Loading of Tower Section

3.1.1. Combination form of Inner and Outer Steel Cladding

In order to quantify the degree of impact of the combination of inner and outer steel cladding on the ultimate bearing capacity of the main member, the difference between the maximum and minimum ultimate loads of the main member corresponding to different combinations of inner and outer steel cladding was calculated for each steel cladding area ratio under different disconnection joint designs. The results are shown in Figure 8. From the figure, it can be seen that the area ratio of the steel cladding is smaller, and the impact of the combination of inner and outer steel cladding on the ultimate bearing capacity of the disconnected main member is greater. In addition to this, when the area ratios of the steel cladding are 1.0 and 1.1, the ultimate bearing capacity of the main member at the middle end disconnection is most affected by the combination form of the inner and outer steel cladding. When the area ratios of the steel cladding are any other values, the ultimate bearing capacity of the upper end disconnection main member is most affected by the combination form of the inner and outer steel cladding. Therefore, it is necessary to study the combination form of the inner and outer steel cladding when designing the steel cladding area ratio.

In this paper, the ultimate loads of three sets of disconnected main members under different combinations of inner and outer steel cladding with different steel cladding area ratios are given. The results are shown in Figure 9. Comparing the ultimate loads of main members under different combinations of inner and outer steel cladding, the optimal working condition is the maximum ultimate load, with a steel cladding area ratio of 0.8 to 1.3. The optimal working conditions, corresponding to the upper end of the main member are A3, B3, C2, D2, E3, and F2, respectively. The optimal working conditions corresponding to the middle end of the main member are A3, B3, C2, D2, E2, and F2, and the optimal

working conditions corresponding to the lower end of the main member are A3, B4, C4, D4, E4, and F4, respectively. All of these optimal operating conditions are explained in Table 1.

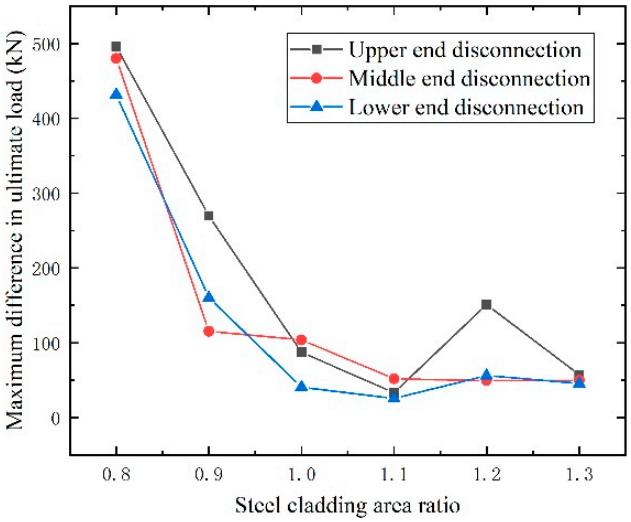

Figure 8. Maximum difference value in ultimate load of different steel cladding combinations under different steel cladding area ratios.

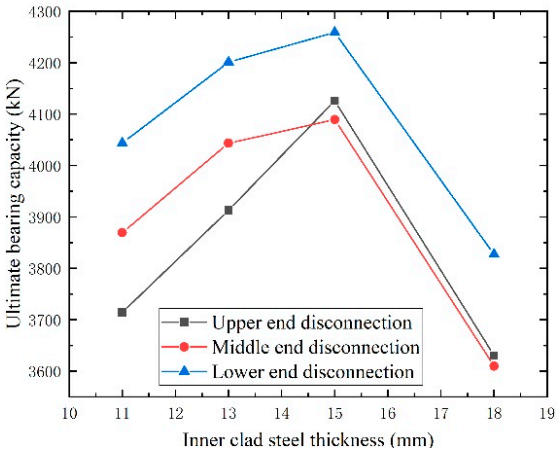

(**a**) Steel cladding area ratio 0.8.

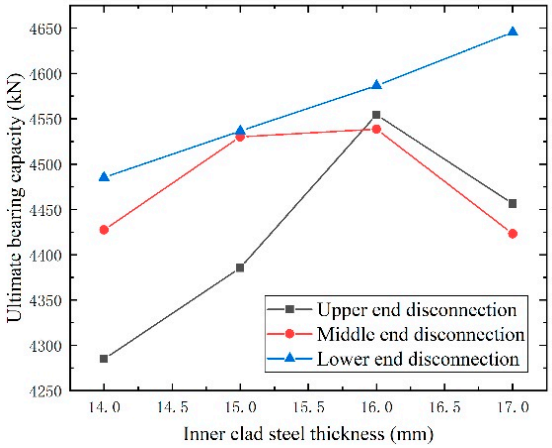

(**b**) Steel cladding area ratio 0.9.

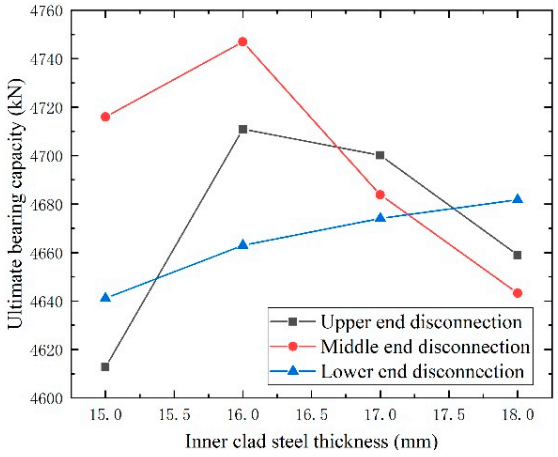

(**c**) Steel cladding area ratio 1.0.

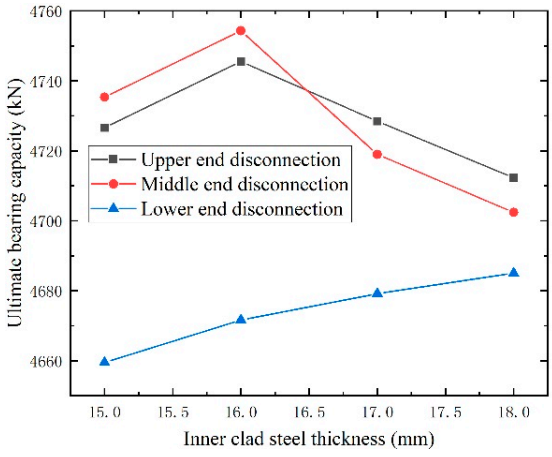

(**d**) Steel cladding area ratio 1.1.

Figure 9. *Cont.*

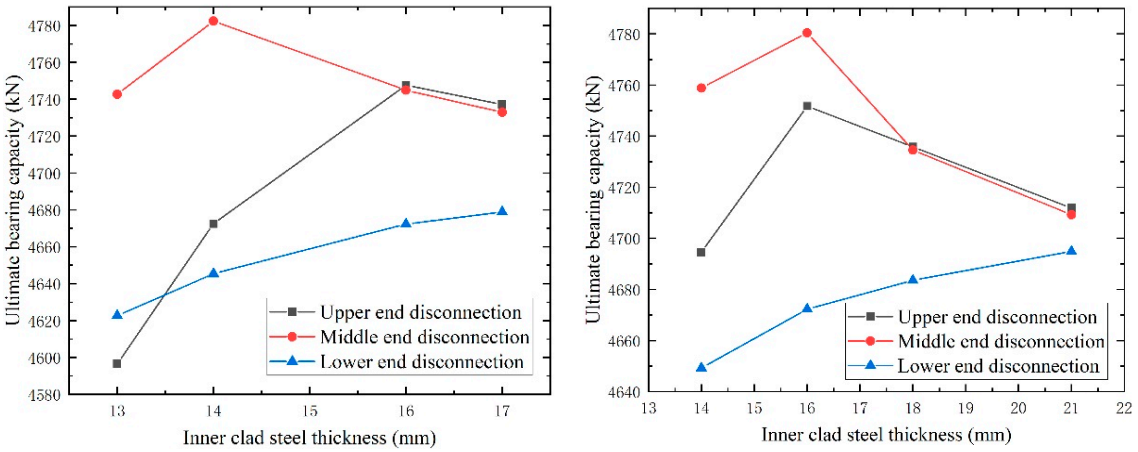

(**e**) Steel cladding area ratio 1.2. (**f**) Steel cladding area ratio 1.3.

Figure 9. Ultimate load of disconnected main members for different steel cladding combination forms.

As shown in Figure 9, the trend in the ultimate loads of the three sets of disconnected main members as the inner steel cladding thickness changes can be observed. It can be found that, considering the same steel cladding area ratio, there are two distinct trends in the ultimate load of the main member: it first increases and then decreases with the increase in inner steel cladding thickness; or it continuously increases with the increase in inner steel cladding thickness. It is observed that the ultimate bearing capacity of the main member can be increased due to a certain degree of increase in the thickness of the inner steel cladding.

3.1.2. Steel Cladding Area Ratio

As shown in Figure 10, it can be seen that the ultimate load of the disconnected main member under the optimal working condition varies with the steel cladding area ratio. Here, the horizontal reference line is the ultimate bearing capacity of the connected main member. As the steel cladding area ratio increases, the ultimate bearing capacity of the main member increases significantly at first, and then slowly, with the steel cladding area ratio to 1.0 as the boundary. Comparing this with the ultimate bearing capacity of the connected main member, it can be found that when the steel cladding area ratio is less than 1.0, the ultimate bearing capacity of the three sets of disconnected main members significantly will decrease. Conversely, when the steel cladding area ratio is greater than or equal to 1.0, the ultimate bearing capacities of the three sets of disconnected main members significantly will increase, and then the ultimate bearing capacities of the middle end disconnected main member will increase to the maximum. Therefore, it is recommended that the middle end of the main member can be chosen as the disconnect position, and the steel cladding area ratio at the disconnection joint can be set at 1.0.

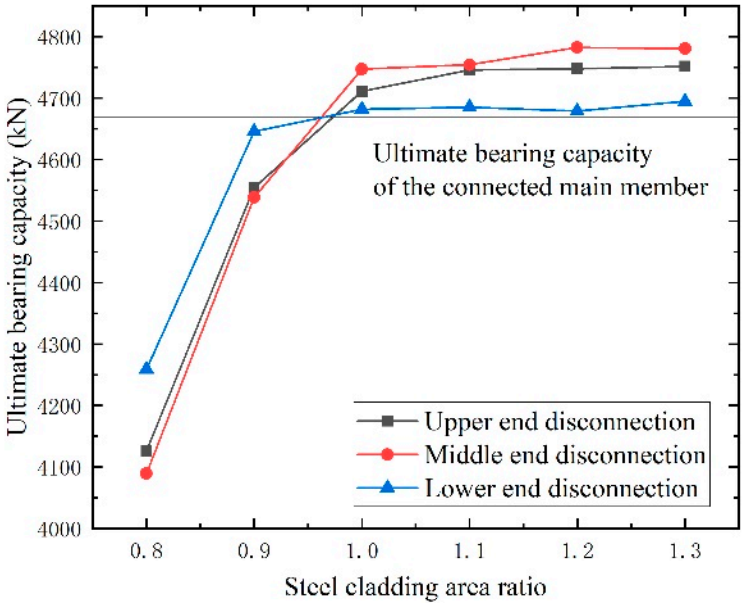

Figure 10. Comparison of ultimate load of main members under different steel cladding area ratios.

3.2. Analysis of Finite Element Results for Tension and Compression Coupled Loading of Tower Section

The out-of-plane displacement (displacement perpendicular to the structural plane) and ultimate thrust at the intersection point of the cross bracing by selecting the optimal working condition and applying tension and compression to the tower section were obtained, as shown in Table 2. As shown in the table, it can be seen that the presence of a disconnecting joint will reduce the stability of the tower section. Furthermore, when there is a disconnection joint in the main member, the layout position of the disconnection joint will have little impact on the stability of the tower section.

Table 2. Out-of-plane displacement of cross bracing.

Type	Steel Cladding Area Ratio	Ultimate Thrust (kN)	Out-of-Plane Displacement (mm)
No disconnection	non	463.6	141.5
Upper end disconnection	0.8	395.4	167.8
	0.9	395.4	167.5
	1.0	395.4	167.4
	1.1	401.2	167.8
	1.2	395.4	168.7
	1.3	395.4	171.0
Mid end disconnection	0.8	401.0	167.7
	0.9	401.0	167.7
	1.0	401.0	167.7
	1.1	401.0	167.7
	1.2	401.0	167.4
	1.3	401.0	167.2
Lower end disconnection	0.8	396.2	165.6
	0.9	396.3	165.6
	1.0	396.3	165.6
	1.1	396.8	165.6
	1.2	396.2	165.6
	1.3	396.4	165.7

3.3. Slenderness Ratio Correction Factor for Disconnection Main Members

The slenderness ratio correction factors for the three types of disconnection main members under various optimal working conditions are calculated based on the principle of slenderness ratio correction, as shown in Figure 11.

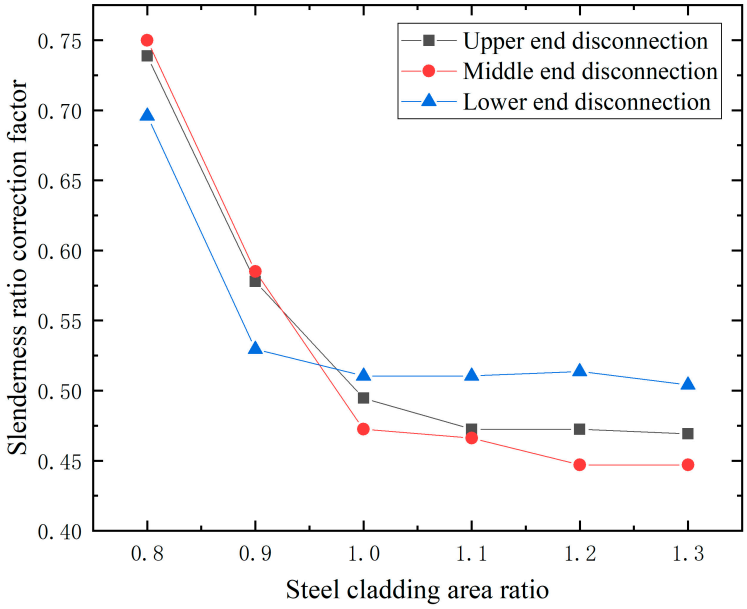

Figure 11. Scatter plot of the slenderness ratio correction factor of the disconnect main member.

From Figure 11, it can be observed that the correction factor decreases with the increase in the steel cladding area ratio, demonstrating a clear inverse proportional relationship. Therefore, the least squares method can be employed to fit the data and obtain the following formula for the slenderness ratio correction coefficient for the disconnected main member at the upper end.

$$K_\lambda = \frac{0.5408}{a} + 0.0082 \tag{4}$$

The slenderness ratio correction coefficient for the disconnected main member at the middle end will be given by Equation (4).

$$K_\lambda = \frac{0.6168}{a} - 0.0758 \tag{5}$$

The slenderness ratio correction coefficient for the disconnected main member at the lower end will be given by Equation (5).

$$K_\lambda = \frac{0.3326}{a} + 0.2185 \tag{6}$$

4. Conclusions

Based on finite element simulation analysis for the four groups of the tower section, the following conclusions were obtained:

(1) Considering the same steel cladding area ratio, the ultimate bearing capacity of the main member will be affected by the combination of internal and external steel cladding on the disconnected joint. Increasing the thickness of the inner cladding will increase the stiffness at the disconnection joint position to a certain extent, thereby enhancing the ultimate bearing capacity of the main member. Therefore, the influence of the combination form of the inner and outer steel cladding on the joint should be considered when designing the disconnection joint in the main member of the transmission tower.

(2) The ultimate bearing capacity of the main member increases significantly at first and then slowly with the steel cladding area ratio set to 1.0 as the boundary. When the area ratio of steel cladding is greater than or equal to 1.0, the disconnection joint can improve the ultimate bearing capacity of the main member. Especially, the most significant improvement in the ultimate bearing capacity of the main member is achieved when the disconnection joint is located at the middle end of the main member. It is recommended that the middle end of the main member can be chosen as the disconnection position, and the steel cladding area ratio at the disconnection joint can be set to 1.0.

(3) The mode of tower section instability is out-of-plane deformation, and the disconnection joint in the main member reduces the stability of the tower section significantly. When there is a disconnection joint in the main member, the stability of the tower section is not affected by the location of the disconnection joint in the main member.

(4) Because the ultimate bearing capacity of the main member is affected by the disconnection joint in the main member, the slenderness ratio correction coefficient formulas have been derived in this paper for the upper end disconnected main member, the middle end disconnected main member, and the lower end disconnected main member.

Author Contributions: Conceptualization, H.Z. and Z.Y.; methodology, H.Z.; software, C.W.; validation, C.W., J.L. and L.Z.; formal analysis, C.W.; investigation, C.W.; resources, C.W.; data curation, C.W.; writing—original draft preparation, H.Z. and C.W.; writing—review and editing, H.Z. and Z.Y.; visualization, C.W., J.L., L.Z. and K.L.; supervision, H.Z. and Z.Y.; project administration, H.Z. and Z.Y.; funding acquisition, Z.Y. All authors have read and agreed to the published version of the manuscript.

Funding: This research was funded by the National Natural Science Foundation of China (Grant No. 11602042 and 11802047), Foundation and Frontier Projects in Chongqing City (Grant Nos. cstc2019jcyj-msxmX0317 and cstc2015jcyjA50010).

Data Availability Statement: The data used to support the findings of this study are included in the article.

Conflicts of Interest: The authors declare no conflicts of interest.

References

1. Shanley, F.R. Inelastic column theory. *J. Aeronaut Sci.* **1947**, *14*, 261–267. [CrossRef]
2. Mengelkoch, N.S.; Yura, J.A. Single-angle compression members loaded through one leg. *Gainesville SSRC* **2002**, 212–218.
3. Liu, Y.; Hui, L. Behavior of steel single angles subjected to eccentric axial loads. *Can. J. Civ. Eng.* **2010**, *37*, 887–896. [CrossRef]
4. Dobri, J.; Filipovi, A.; Baddoo, N. Design procedures for cold-formed stainless steel equal-leg angle columns. *Thin-Walled Struct.* **2020**, *159*, 107210. [CrossRef]
5. Fasoulakis, Z.C.; Lignos, X.A.; Avraam, T.P.; Katsatsidis, S.P. Investigation on single-bolted cold-formed steel angles with geometric imperfections under compression. *J. Constr. Steel Res.* **2019**, *162*, 265–278. [CrossRef]
6. Iftesham, B.; Mahmud, K.A. Comparison of Codes for Axial Compression Capacity of Eccentrically Loaded Single Angles. *J. Constr. Steel Res.* **2021**, *185*, 106829.
7. Giacomo, V.; Zongchen, L.; Christian, A. Evaluation of the Ultimate Collapse Load of a High-Voltage Transmission Tower under Excessive Wind Loads. *Buildings* **2023**, *13*, 513. [CrossRef]
8. Wang, J.; Qi, H.; Zhang, Z.; Zhang, B.; Sun, Q. Failure mechanism of a Q690 steel tubular transmission Tower: Full-Scale experiment and numerical simulation. *Eng. Struct.* **2023**, *295*, 116881. [CrossRef]
9. Shen, G.; Yu, H.; Yu, L.; Li, B.; Yao, J. Seismic responses of a long-span transmission tower and tower-line system. *J. Phys. Conf. Ser.* **2022**, *2351*, 012023. [CrossRef]
10. Deng, Z.H.; Huang, B. Study on ultimate bearing capacity of main member in transmission tubular tower leg. *Thin-Walled Struct.* **2018**, *127*, 51–61. [CrossRef]
11. Li, R.; Qi, L.; Dong, Y.-R.; Wang, H. Nonlinear Performance of Steel Tube Tower in Ultra-High Voltage Transmission Lines under Wind Loads. *Buildings* **2024**, *14*, 140. [CrossRef]
12. Kim, P.; Han, W.S.; Kim, J.H.; Lee, J.; Kang, Y.J.; Kim, S. Analytical Investigation of the Effects of Secondary Structural Members on the Structural Behaviors of Transmission Towers. *Buildings* **2023**, *13*, 223. [CrossRef]
13. *DL/T 5154-2012*; Technical Code for the Design of Tower and Pole Structures of Overhead Transmission Line. China Planning Press: Beijing, China, 2012. (In Chinese)

14. *GB50017-2017*; Steel Structure Design Standards. China Construction Industry Press: Beijing, China, 2017. (In Chinese)
15. Fan, G. Research on the Stability Capacity of the Equal Angle Steel Main Member in Transmission Tower Considering Middle Disconnected Joint. Master's Thesis, Chongqing University, Chongqing, China, 2021. (In Chinese)
16. Xue, S.; Wang, L.; Li, X.; Zhou, Y. Finite element analysis of axial pressure stability bearing capacity of angle steel such as transmission tower. *Build. Struct.* **2023**, *53* (Suppl. 1), 1431–1435. (In Chinese)
17. Ma, L.; Bocchini, P. Hysteretic Model of Single-Bolted Angle Connections for Lattice Steel Towers. *J. Eng. Mech.* **2019**, *145*, 04019052. [CrossRef]
18. Mahmoudi, M.; Kosari, M.; Lorestani, M.; Abad, M.J. Effect of contact surface type on the slip resistance in bolted connections. *J. Constr. Steel Res.* **2020**, *166*, 105943. [CrossRef]
19. Poovakaud, V.V.; Jiménez-Peña, C.; Talemi, R.; Coppieters, S.; Debruyne, D. Assessment of fretting fatigue in high strength steel bolted connections with simplified Fe modelling techniques. *Tribol. Int.* **2020**, *143*, 106083. [CrossRef]
20. Abdelrahman, A.H.A.; Liu, Y.; Chan, S. Advanced joint slip model for single-angle bolted connections considering various effects. *Adv. Struct. Eng.* **2020**, *23*, 2121–2135. [CrossRef]
21. de Souza, R.R.; Miguel, L.F.; Kaminski, J., Jr.; Lopez, R.H.; Torii, A.J. Optimization of transmission towers considering the bolt slippage effect. *Eng. Struct.* **2020**, *211*, 110436. [CrossRef]
22. Abad, J.; Franco, J.M.; Celorrio, R.; Lezáun, L. Design of experiments and energy dissipation analysis for a contact mechanics 3D model of frictional bolted lap joints. *Adv. Eng. Softw.* **2012**, *45*, 42–53. [CrossRef]
23. Huang, Z.; Liu, H.; Zhang, J.; Li, Z.; Ohsaki, M.; Bai, Q. Experimental and numerical study on the effective length of tower cross bracing. *Thin-Walled Struct.* **2023**, *182*, 110296. [CrossRef]
24. Li, J.; Li, Z.; Huang, X.; Liu, H.; Wang, W. Study on the influence of restraint stiffness of main material on the compression stability bearing capacity of cross-bracing in transmission tower. *J. Phys. Conf. Ser.* **2022**, *2260*, 012004. [CrossRef]
25. Tang, Z.; Li, Z.; Wang, T. Probabilistic bearing capacity assessment for unequal-leg angle cross-bracings in transmission towers. *J. Constr. Steel Res.* **2023**, *200*, 107672. [CrossRef]
26. Li, Y.; Yan, Z.; Zhou, D.; Ren, Q.; Hua, C.; Zhong, Y. Analysis of the stability behavior of cross bracings in transmission towers based on experiments and numerical simulations. *Thin-Walled Struct.* **2023**, *185*, 110554. [CrossRef]
27. Li, Y. Theoretical and Experimental Study on Bearing Capacity of Unequal Angle Steel in Transmission Tower. Ph.D. Thesis, Chongqing University, Chongqing, China, 2017. (In Chinese)